A Biased Anode to Suppress Ion Back-Bombardment in a DC High Voltage Photoelectron Gun

J. Grames[a], P. Adderley[a], J. Brittian[a], J. Clark[a], J. Hansknecht[a], D. Machie[a], M. Poelker[a], E. Pozdeyev[b], M. Stutzman[a], K. Surles-Law[a]

[a]*Thomas Jefferson National Accelerator Facility, 12000 Jefferson Avenue, Newport News, Virginia 23606*

[b]*Brookhaven National Laboratory, Upton, New York 11973-5000*

Abstract. Ion back-bombardment is the dominant mechanism that limits the operating lifetime of DC high voltage GaAs photoelectron guns. In this work, an electrically isolated anode electrode was used to distinguish the QE damage contributions of ions produced within the cathode/anode gap and those produced downstream of the anode. This new anode design provides a means to suppress QE decay due to ionized gas in the beam line.

Keywords: electron source, photocathode
PACS: 29.25.Bx, 85.60.Ha

INTRODUCTION

The production of spin polarized electrons by photoemission from gallium arsenide (GaAs) within DC high voltage guns is a widely accepted technology at accelerators devoted to nuclear and high energy physics research [1]. The same technology can be used to create unpolarized electron beams for light sources [2], electron coolers [3] and positron drivers [4]. Many of these GaAs photogun applications share challenging high average current beam requirements that extend beyond today's state of the art. In particular, a fundamental concern is the ability to sustain high quantum efficiency (QE) over sufficiently long periods of time at milliAmpere beam current.

Ion back-bombardment is the dominant mechanism that limits the operating lifetime of DC high voltage GaAs photoelectron guns. Residual gas originates from outgassing of the vacuum chamber walls and from electron stimulated desorption associated with inadvertent beam loss along the beam line. The gas, if ionized by the primary electron beam, can be accelerated back toward the photocathode acquiring kinetic energy from the cathode/anode gap potential. Ultimately, ions striking the photocathode may either sputter away the surface chemicals used to create a negative electron affinity condition or become implanted into the bulk. Both are possible mechanisms for decreasing photocathode quantum efficiency.

The kinetic energy distribution of ions reaching the photocathode depends upon where the ions originate. Residual gas ions created within the cathode/anode electrode gap are accelerated toward the photocathode with kinetic energy *up to the full gun voltage.* Residual gas ions created in the beam line downstream of the anode can migrate into the cathode/anode gap, and are consequently accelerated toward the photocathode with kinetic energy *of the full gun voltage*. This is depicted in Fig. 1 for a laser beam incident off-axis from the photocathode center. Photoemitted electrons are accelerated and focused toward the geometric center of the gun by the electrostatic properties of the cathode/anode gap. Ions created by the electron beam are accelerated toward the photocathode, yet follow a ballistic trajectory owing to a much greater mass. A consequence is that the spatial distribution of ions reaching the photocathode is spread along a line that connects the laser beam location and the electrostatic center of the photocathode. Low energy ions created near the photocathode surface arrive at the photocathode near the location of the laser beam, whereas ions created near the anode or beyond, are delivered to the center of the photocathode. This phenomenon, referred to as ion trenching (see Fig. 1) has been reported previously [5].

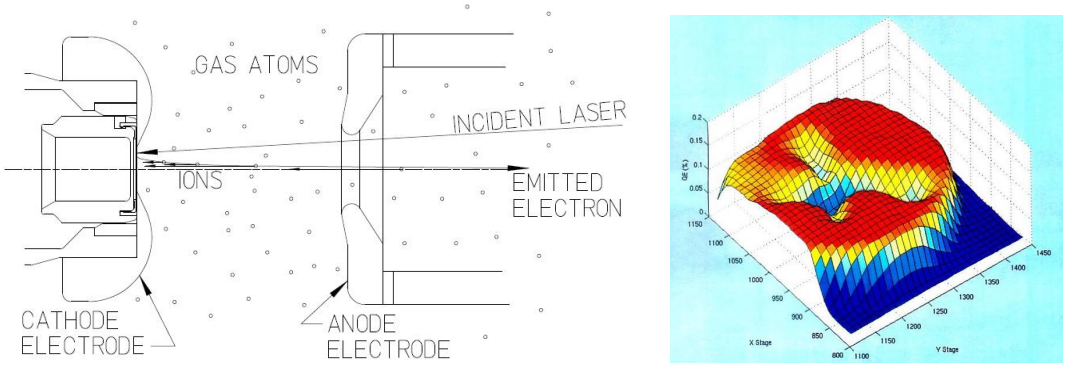

FIGURE 1. Left: Illustration showing photoemitted electrons and ion back-bombardment for off-axis illumination of photocathode and Right: a plot of QE across the surface of the photocathode that has been damaged by ions; electron beam was extracted from three different radial locations. Note QE "trenches" that terminate at a common "electrostatic center".

Ultimately, the rate of ion bombardment at the photocathode is determined by electron beam current, residual gas pressure and the electron impact ionization cross section for each residual gas species. The ionization cross section for molecular hydrogen (the dominant gas species in DC photoguns) as a function of electron beam is calculated [6] and shown in Fig. 2. Clearly, ion production occurs most plentifully at lower beam energies, which corresponds to the location very near the photocathode however this location also corresponds to very good vacuum. Whereas, downstream of the anode, despite significantly smaller ionization cross section, it is possible that many more ions are produced because vacuum is not as good compared to conditions within the gun. For typical photoguns the ion production rate is about 10^6-10^7 ions/C both within the gap *and* downstream of the anode. In the past, the contribution of ions created downstream of the gun anode has been ignored. Recent efforts begun at Jefferson Laboratory (JLab) have tried to distinguish the two. Specifically, estimates of ion trapping in DC photoguns and a concept to limit those produced downstream of the anode have been published [7]. In this paper, experimental investigation of a biased anode for limiting damaging ions is presented.

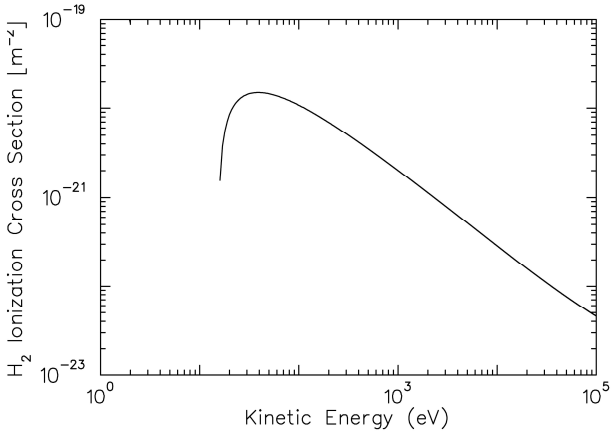

FIGURE 2. Electron impact ionization cross section for H_2 as a function of electron kinetic energy.

BIASED ANODE DESIGN

A new DC high voltage (100 kV) load lock GaAs photogun has been constructed at JLab, with improved vacuum and photocathode preparation capabilities. This gun was previously used to study photocathode lifetime with bulk GaAs at DC beam currents to 10 mA [8] and high polarization strained layer superlattice GaAs at 1 mA [9].

To accomplish the tests reported here the photogun high voltage chamber (Fig. 3a) was modified to electrically isolate the anode electrode and anode support tube from the grounded vacuum chamber, each independently connected to a power supply via a vacuum electrical feed-through. The code POISSON [10] was used to model the electrostatic potential of the gun chamber for both the conventional (anode electrode = anode support = 0 V) and biased (anode electrode = +2000V, anode support = +300V) configurations (Fig. 3b).

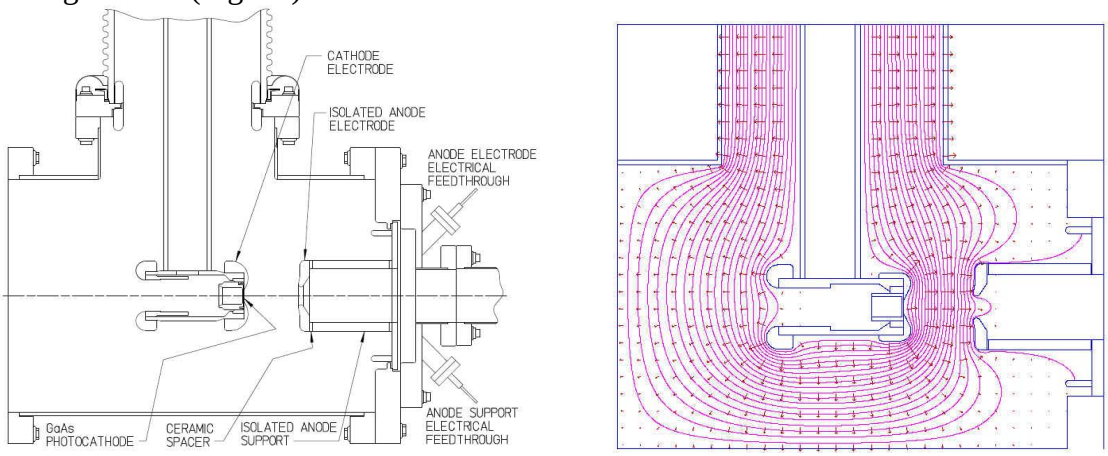

FIGURE 3. (a) Modified high voltage chamber assembly and (b) POISSON model showing equipotentials for the biased anode configuration.

The electrostatic potential along the electron gun axis is shown for both configurations in Fig. 4. Plot (a) shows a coarse y-axis while plot (b) shows finer resolution. Notice the grounded anode configuration attracts positive ions entering the gun chamber, whereas the biased configuration produces a potential barrier of +425 V,

which ions must overcome to enter the cathode/anode gap. This barrier significantly exceeds the kinetic energy of ions trapped within the potential of the electron beam [7]. The final electron energy for both configurations is 100 keV.

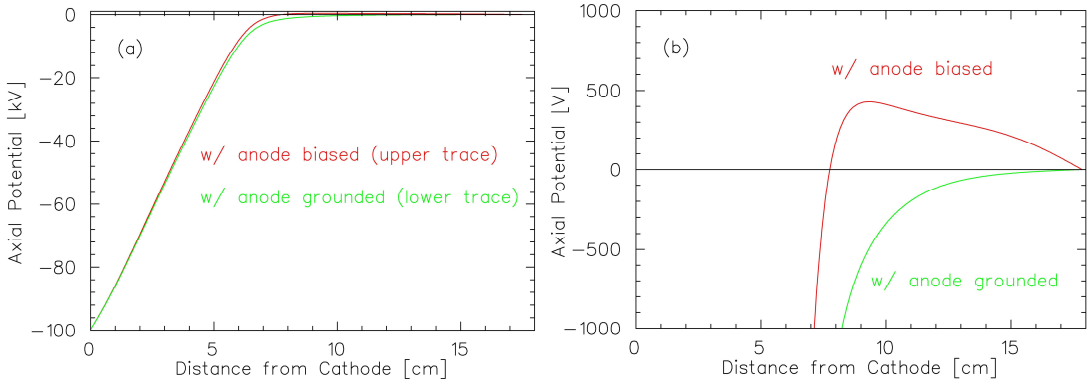

FIGURE 4. (a) The potentials on the electron gun axis from cathode (0 cm) to anode (~6 cm) to gun exit (~18 cm) are similar; however, a finer resolution plot (b) clearly illustrates the attractive potential well of the grounded configuration from the "potential barrier" behavior of the biased configuration.

TEST STAND COMMISSIONING

The test stand layout for photocathode lifetime studies is shown in Fig. 5 and was described previously in references 8 and 9. Bulk GaAs with DC green-light illumination was used for these tests. The photocathode active area was 5 mm with a focused drive laser spot 0.37 mm diameter FWHM. The QE across the photocathode surface was recorded by biasing the photocathode at low voltage and measuring photoemission as the laser beam was scanned across the photocathode. A "QE scan" of the photocathode is shown in Fig. 6 (left) with QE nearly uniform across the active area and maximum value ~10%.

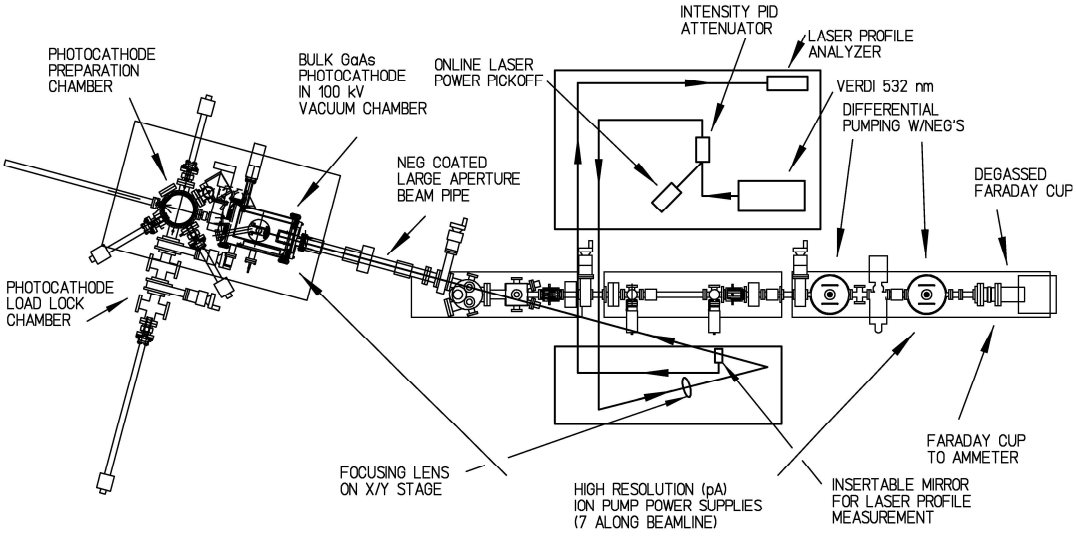

FIGURE 5. The 100 kV GaAs photogun, beam line and laser system is shown. The location of the first solenoid magnet (midway on the NEG-coated beam line) likely defines the extent of the region downstream of the anode that contributes to QE decay from ion back-bombardment.

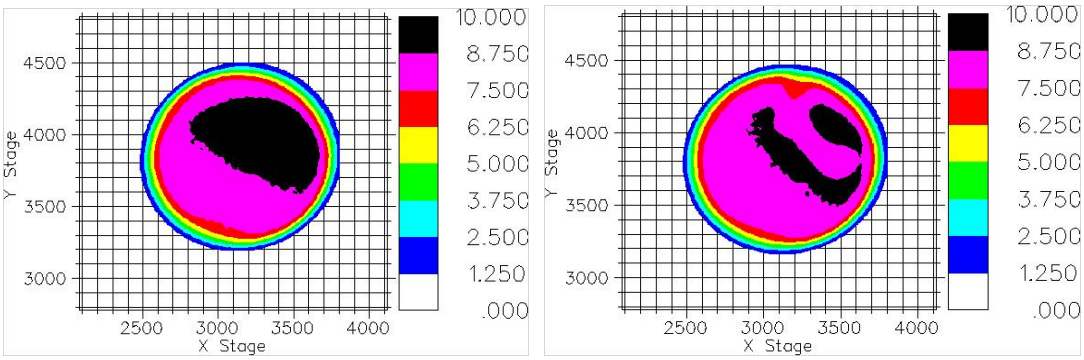

FIGURE 6. Left: Initial photocathode QE, before running beam, with active area of 5 mm and Right: QE scan after extracting beam, demonstrating ion back-bombardment and providing experimental determination of the electrostatic center.

To distinguish QE damage associated with ions created within the cathode/anode gap from those created downstream of the anode, the laser spot was moved about ~1.8 mm from the electrostatic center (EC), corresponding to a stepper motor location x=3100, y=3700 [11]. Two runs were made, each with beam current 5 mA and total extracted charge ~175 C, first with the anode biased and then grounded. High resolution QE scans of the photocathode region that includes the laser spot (i.e., origin of beam) and the EC were obtained at the beginning and end of each run to quantify QE decay. QE ***difference*** plots, between final and initial QE, are shown in Fig. 7, where the color-coded axis corresponds to QE lost during the run. For the grounded anode configuration (Fig. 7a), there is clear evidence of trenching, with ion damage distributed from the laser spot (x=3100, y=3700) toward the electrostatic center (x=3000, y=4000). In the case of the biased configuration (Fig. 7b) the damage at the EC is significantly reduced. Note the 1/e photocathode lifetime at the laser spot (~60 stepper motor units FWHM) is about 340 C for both configurations.

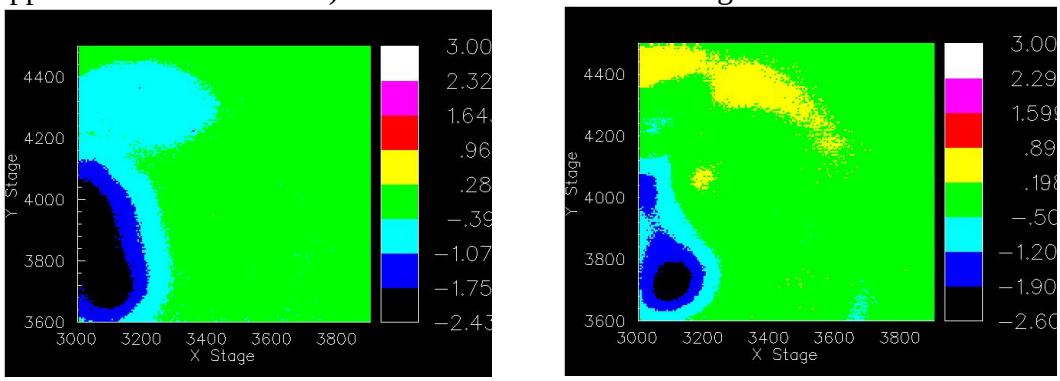

FIGURE 7. Difference plots between final and initial QE for both the (a) grounded configuration and (b) biased anode configurations. Here, the color-coded axis corresponds to QE lost during the run. Note, the scans are of higher resolution, and consequently a smaller region was mapped, compared to those in Fig. 6 showing the entire photocathode.

In another test the laser beam was moved to the electrostatic center (x=3000, y=4000) so that all of the ions generated by the beam, including those within the cathode/anode gap and those downstream of the anode would accumulate at the EC. The photocathode lifetime (1/e reduction of QE) was measured at a beam current of 2 mA with the anode alternately biased and grounded. The results (Fig. 8) suggest the

biased configuration yields an improved lifetime. Averages of the biased and grounded results indicate charge lifetime improved ~22% at the EC, using the biased anode configuration (note when considering all four data points, there appears to be an overall trend toward reduced charge lifetime, and this may be a result of slight vacuum degradation encountered over the duration).

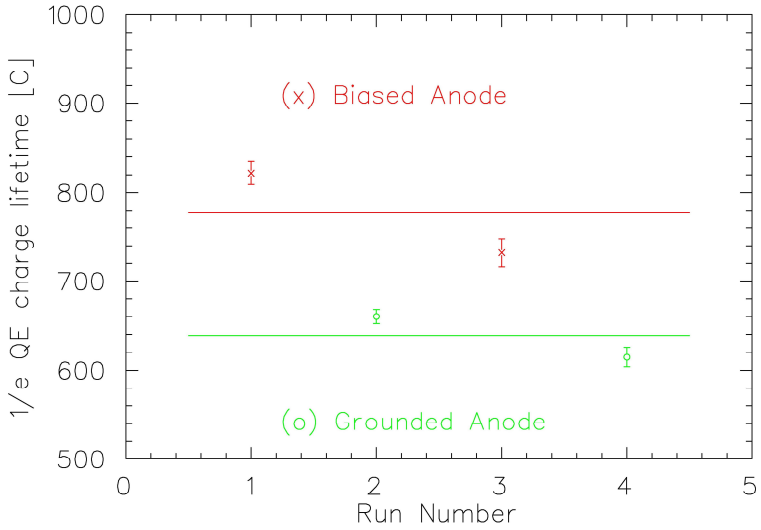

FIGURE 8. Photocathode 1/e QE charge lifetime at 2 mA for alternately biased and grounded anode; the average for both the biased and grounded configurations is shown with the horizontal bars.

For comparison, the rate of ion production (or yield) was calculated using the cross section for H_2 shown in Fig. 2, assuming a uniform pressure within the gun and beam line of 8×10^{-12} Torr and the gun potentials shown in Fig. 4. The ion yield at each location along the beam line is shown in Fig. 9 (left) and the cumulative ion yield is shown in Fig. 9 (right), up to the first solenoid magnet which likely defines the extent of the region downstream of the anode that contributes to QE decay from ion back-bombardment [7].

For the grounded anode case, assume all of the ions created in the gun chamber (2.9×10^7 ions/C) and those extending to the first solenoid (2.4×10^7 ions/C) reach the photocathode; a total of 5.3×10^7 ions/C. For the biased anode case, assume only the ions created in the gun chamber up to the peak of the potential barrier (about 9 cm from the photocathode) reach the photocathode; a total of 2.2×10^7 ions/C. The ratio of ion production suggests the biased anode should enhance QE lifetime by ~58% compared to ~22% observed experimentally. If however, one limits the region of relevant ion production to the end of the gun vacuum chamber (~18 cm from the photocathode), instead of extending to the first solenoid, a comparison of ion yield for the two configurations suggests the biased anode should enhance QE by ~24%, much closer to the measured result. Uncertainty about the actual mechanics of ion trapping by the beam, combined with uncertainty of the ion energy dependence relating to QE damage, makes it difficult to predict the magnitude of lifetime enhancement.

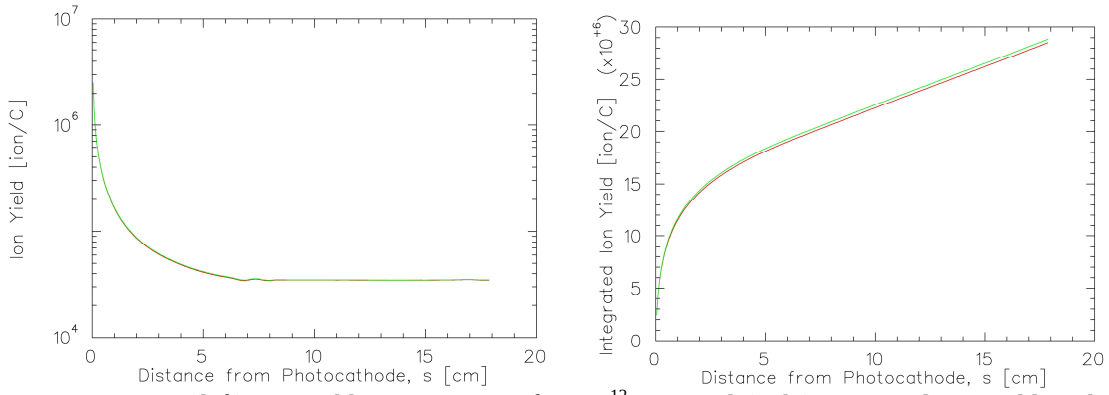

FIGURE 9. (left) Ion yield at a pressure of 8×10^{-12} Torr and (right) integrated ion yield in the electron gun high voltage chamber for both the biased and grounded anode configurations; note the similar electrostatic potentials have nearly identical ion yields.

CEBAF COMMISSIONING

The load lock gun was recently installed at CEBAF with the anode biased as described above. To date, insufficient beam has been extracted from the new gun to determine if the biased anode provides enhanced photocathode lifetime, but measurements were performed to compare beam transport properties for the grounded and biased configurations. After biasing the anode, no change was observed in beam line vacuum or orbit (resolution ~ 0.1 mm). The beam transverse size increased by ~2%, as measured using a wire scanner (see Table 1). This is likely due to a change in the electrostatic cathode/anode lens strength and will be modeled later. Electron bunch profile was measured using a slit scanning method: the bunch temporal profile was unchanged, but the transit time to the analyzer reduced by about ~8 ps (see Fig. 10a). This reduction in time-of-flight was confirmed (Fig. 10b) mathematically using the potentials shown in Fig. 4. Overall, the slight modifications to electron beam characteristics related to the biased anode appear entirely manageable for CEBAF.

TABLE 1. Measured beam size for both grounded and biased anode.

Measured Parameter	Grounded	Biased
Horizontal beam width, σ_x (mm)	0.208 ± 0.002	0.213 ± 0.002
Vertical beam width, σ_y (mm)	0.199 ± 0.003	0.205 ± 0.002

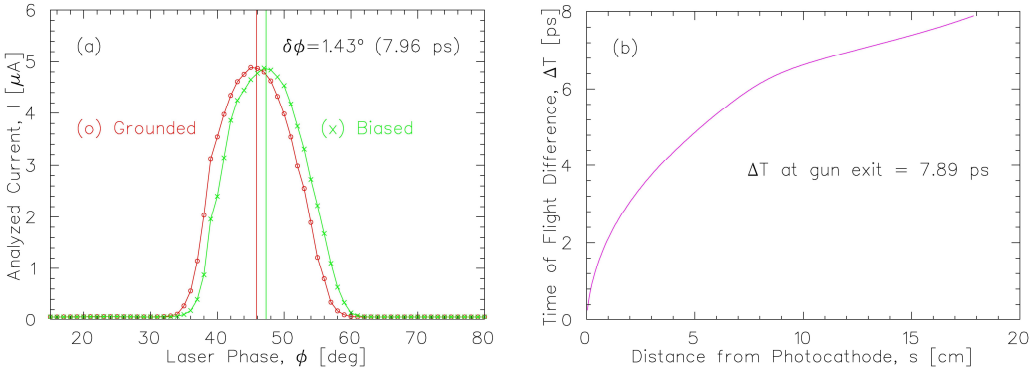

FIGURE 10. (a) Measured longitudinal bunch profile and (b) simulated difference between the biased and grounded anode configurations indicate an 8 ps earlier arrival time agree.

SUMMARY

In this work, a DC photogun with a biased anode was used to distinguish the QE damage contributions of residual gas ionized within the cathode/anode gap from that produced downstream of the anode. This new biased anode design provides a means to suppress photocathode QE damage located at the electrostatic center. This is particularly important for photoguns that cannot avoid extracting beam from the EC, in particular high intensity photogun applications that require a large laser spot size, e.g., to extend photocathode lifetime [12] or to manage surface charge limitation by reducing photocathode current density. Finally, modulating the anode bias voltage may be useful to adjust the beam arrival time or spot size easily, e.g., correlated with the beam helicity of polarized electron photoguns used in parity violating experiments.

ACKNOWLEDGMENTS

The authors would like to acknowledge useful discussions with Charles Sinclair and contributions by Jonathan Dumas. This manuscript has been authored by Jefferson Science Associates, LLC under U.S. DOE Contract No. DE-AC05-06OR23177. The U.S. Government retains a non-exclusive, paid-up, irrevocable, world-wide license to publish or reproduce this manuscript for U.S. Government purposes.

REFERENCES

1. C. K. Sinclair et al., Phys. Rev. Special Topics Accelerator and Beams **10**, 023501 (2007).
2. I. Bazarov et al., in Proc. of the 2002 European Particle Accelerator Conference, Paris, France.
3. I. Ben-Zvi et al., in Proceedings of the 2007 Particle Accelerator Conference, WEOCKI03, p. 1938.
4. S. Golge et al., in Proceedings of the 2007 Particle Accelerator Conference, THPMS067, p. 3133.
5. K. Aulenbacher et al., SLAC Report 432 (1993).
6. M. Reiser, Theory and Design of Charged Particle Beams, John Wiley & Sons, Inc. (1994).
7. E. Pozdeyev, Phys. Rev. ST-AB 85, p. 2503-2504 (2007).
8. J. Grames et al., in AIP Conference Proceedings 915, p. 1037-1044 (2006).
9. J. Grames et al., in Proceedings of the 2007 Particle Accelerator Conference, THPMS064, p. 3130.
10. K. Halbach and R. Holsinger, Particle Accelerators 7, 21 (1976); see http://laacg1.lanl.gov/.
11. Note the electrostatic center does not always correspond to the geometric center of the photocathode active area. Small misalignment may result due to assembly misalignment of the cathode/anode electrodes and location of the activation mask used to limit the active area of the photocathode.
12. J. Grames et al., work to be published.